Pincer-based heterobimetallic Pt(II)/Ru(II), Pt(II)/Ir(III) and Pt(II)/Cu(I) complexes: synthesis and evaluation antiproliferative properties

Benoit Bertrand, Geoffrey Gontard, Candice Botuha, Michèle Salmain

Pincer-based heterobimetallic Pt(II)/Ru(II), Pt(II)/Ir(III) and Pt(II)/Cu(I) complexes: synthesis and antiproliferative properties evaluation

Benoît Bertrand,[a]* Geoffrey Gontard,[a] Candice Botuha[a] and Michèle Salmain[a]

[a] Sorbonne Université, CNRS, Institut Parisien de Chimie Moléculaire (IPCM), F-75005 Paris, France

Corresponding author e-mail address: benoit.bertrand@sorbonne-universite.fr

Abstract

Platinum pincer-based complexes [(O^N^O)Pt(L)] (L = DMSO, pyridine, triphenylphosphine or 1,3-dimethylbenzimidazol-2-ylidene) carrying an (N^N) coordination site were used as starting materials to synthesize a series of seven cationic heterobimetallic Pt(II)/Ru(II), Pt(II)/Ir(III) and Pt(II)/Cu(I) presenting a [(*p*-cymene)RuCl]$^+$, a [(Cp*)IrCl]$^+$ (Cp* = η^5-pentamethylcyclopentadienyl) and a [(NHC^{iPr})Cu]$^+$ (NHC^{iPr} = 1,3-bis(2,6-diisopropylphenyl)imidazole-2-ylidene) moiety respectively. The X-ray structure of one of the bimetallic Pt(II)/Ir(III) complexes showed a distortion of the organic platform to accommodate the coordination geometry of both metal centers as already observed for previous Pt(II)/Re(I) complexes. The antiproliferative activity of the complexes was first screened on the triple negative breast cancer cell line MDA-MB-231. Then the IC_{50} of the most active candidates was determined on a wider panel of human cancer cells (MDA-MB-231, MCF-7 and A2780) as well as on a non-tumorigenic cell line (MCF-10A). The most toxic compound, namely the Pt(II)/Cu(I) heterobimetallic complex **4c** showed an antiproliferative activity down to the nanomolar level.

Introduction

Since the end of the 70's, platinum-based drugs are the standards of care for many types of cancers including, testicular, bladder, melanomas and lymphomas.[1] However, despite their indisputable successes in the clinic, only few platinum complexes have reached worldwide approval. This is mainly due to the heavy side effects induced by these drugs thus dramatically limiting the doses given to patients. This limitation has been one of the major causes of rejection of platinum-based drug candidates in clinical trials.[2] To overcome these limitations, one promising strategy that has emerged is the concept of « multinuclearity » which associates several metals in a single molecular entity in order to improve the efficacy of the drugs. Within this frame, heterobimetallic complexes could be very promising.[3-9] In

particular, Pt(II) complexes have been associated with various other metal ions such as Au(I),[5] Pd(II),[6] Cu(II),[7] Ru(II)[8] and Re(I).[9] Some examples are depicted in figure 1.

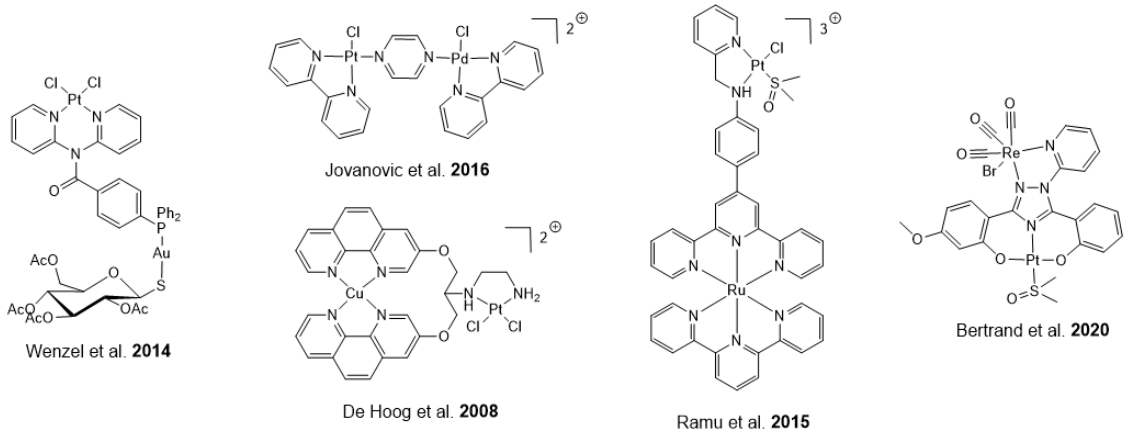

Figure 1: Examples of platinum(II)-based heterobimetallic complexes investigated for anticancer applications.

In some cases, no real improvement in the biological properties resulted from the association of two metals in a single entity as for the Pt(II)/Au(I) complex depicted in figure 1.[5] However, in some other cases, cooperative effects could be observed between the two metals. Indeed, for a Pt(II)/Cu(II) complex (figure 1), the authors observed copper-induced DNA cleavage in the surroundings of GG sequences due to the specific coordination of the Pt(II) moiety to these sequences.[7] Another interest of heterobimetallic complexes is the design of theranostic agents.[10] In this case, one metal will act as the active principle and the second one will be used for luminescence[11] or MRI[12] detection.

In all cases, to ensure the highest synthetic yields, one cannot count on statistics as it is mainly done for homopolymetallic complexes,[13] but rather on the design of orthogonal ligands allowing sequential introduction of the metals[14] or on metal complexes carrying a grafting function for later introduction of the second coordination site or metal complex.[15]

Very recently, we synthesized a series of Pt(II)/Re(I) complexes with very high yield from a central deferasirox-like (N^N)/(O^N^O) bis-chelating ligand by sequential introduction of the Pt(II) and Re(I) ions. We could demonstrate that the observed cytotoxicity solely arose from the [(O^N^O)Pt] fragment, and took advantage of the IR-active [$Re(CO)_3$] fragment to measure the intracellular uptake of our compounds.[9] Based on these results, we have further used the [(O^N^O)Pt(L)] scaffold to introduce Ru(II), Ir(III) and Cu(I) entities which have been demonstrated to possess anticancer activities on their own.[16-18] These new platinum-based heterobimetallic complexes presenting a [(*p*-cymene)RuCl]$^+$, a [(Cp*)IrCl]$^+$ and a [(NHC^{iPr})Cu]$^+$ fragment have been screened for their antiproliferative properties against a « triple negative » human breast cancer cell line (MDA-MB-231). The IC_{50} of the most active candidates has then been determined on a larger panel of cell lines including

breast cancer cell lines (MDA-MB-231 and MCF-7), an ovarian cancer cell line (A2780) and a human non-cancerous cell line (MCF-10A) for comparison.

Results and discussion

Synthesis and characterization

The platinum(II) complexes **1a-d** were synthesized by a two- or three-step procedure following a methodology we previously reported.[9] Taking advantage of the free triazole-pyridine (N^N) ligand, we adapted a procedure used for the synthesis of Au(I)/Ru(II) complexes[19] to synthesize the Pt(II)/Ru(II) complexes **2a-d** by reacting the platinum complexes **1a-d** with the ruthenium dimer $[(p\text{-cymene})RuCl_2]_2$ at room temperature with very high yields (80-87 %). This synthetic procedure is depicted in scheme 1.

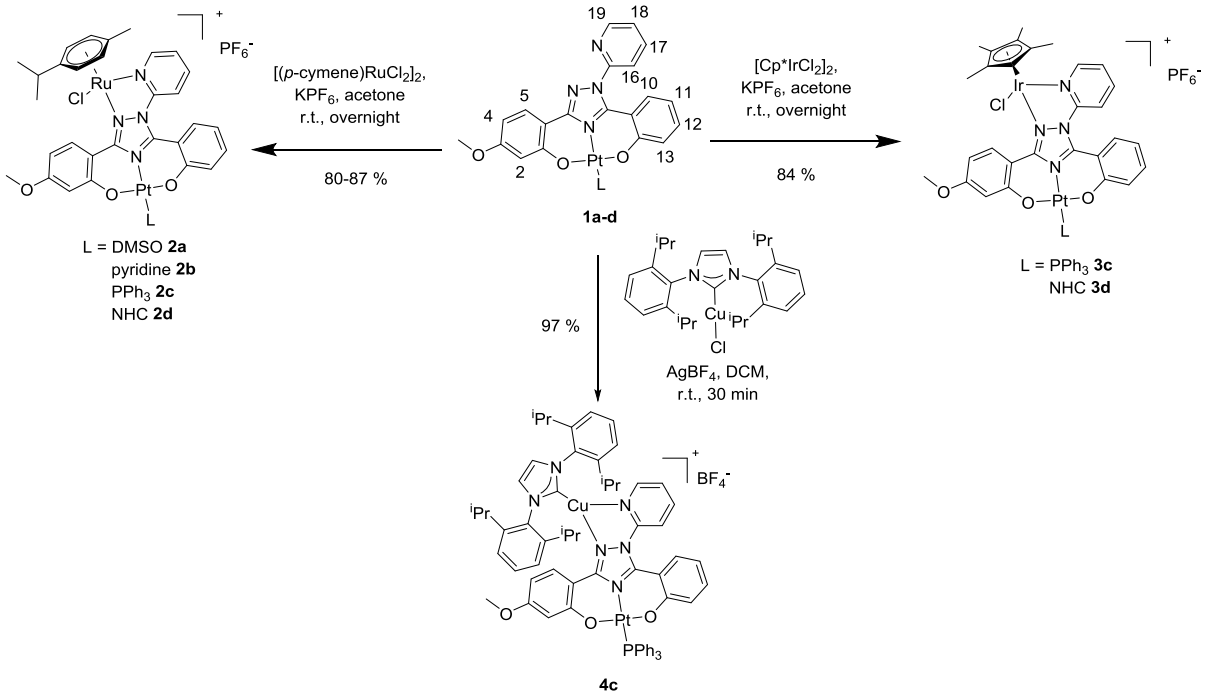

Scheme 1: Synthesis of the heterobimetallic Pt/Ru, Pt/Ir and Pt/Cu complexes.

We could assess the coordination of the $[(p\text{-cymene})RuCl]^+$ fragment to the (N^N) chelate by ^1H NMR spectroscopy. Indeed in the ^1H NMR spectra of the Pt(II)/Ru(II) complexes **2a-d**, we observed a deshielding of around 0.3 ppm and of around 1 ppm for the signals corresponding to H^{19} and H^5 respectively (see scheme 1 for numbering). Moreover, upon coordination of the $[(p\text{-cymene})RuCl]^+$ fragment to the unsymmetrical (N^N) chelate, the Ru(II) ion turned into a stereogenic center which made the two methyl of the isopropyl group magnetically inequivalent in the Pt(II)/Ru(II) complexes as well as the two methyl groups of the DMSO ligand in complex **2a**. This is visible on the ^1H NMR spectrum of **2a**

where the two methyl groups of DMSO appear as two singlets integrating for 3 protons each at 3.45 and 3.41 ppm respectively.

In the same way, by reacting the platinum(II) complexes **1c-d** with the iridium dimer $[(Cp^*)IrCl_2]_2$, we obtained the heterobimetallic complexes Pt(II)/Ir(III) complexes **3c-d** in 84 % yield in both cases (scheme 1). Although no quantitative comparison between the chemical shifts of the ^1H NMR signals of the Pt(II)/Ir(III) complexes **3c-d** and their Pt(II) precursors **1c-d** could be made due to different NMR solvents used for analysis (CD_3CN for **3c-d** and $CDCl_3$ for **1c-d**), we observed a large deshielding of the signal of H^5 , even more than the signal of H^{19}, in both cases. This is good agreement with what we already observed in the case of the Pt(II)/Ru(II) complexes **2a-d**. This feature may be explained by the fact that for the heterobimetallic complexes Pt(II)/Ir(III) and Pt(II)/Ru(II), H^5 is placed for geometrical reasons in the deshielding cone of the aromatic ligand of either the Ir(III) or the Ru(II) atom.

Starting from (1,3-(2,6-(^{i}Pr)$_2$C$_6$H$_3$)$_2$imdazol-2-ylidene)CuCl, after chloride abstraction using $AgBF_4$ and subsequent reaction with **1c** at room temperature, the heterobimetallic Pt(II)/Cu(I) **4c** was obtained in very high yield (scheme 1). The formation of the heterobimetallic complex **4c** was assessed by ^1H NMR spectroscopy. Indeed, in the ^1H NMR spectrum of **4c**, the signal corresponding to H^{19} is broadened due to the steric hindrance brought by the isopropyl groups. Moreover, we observed two sets of signals for the isopropyl groups indicative of a restricted rotation around the C-Cu bond due to the steric hindrance of the triazole-pyridine ligand. Although no crystal structure could be obtained for complex **4c**, we assume a planar trigonal geometry of the Cu(I) cation by analogy with previously reported $[(NHC)Cu(N\hat{}N)]^+$ complexes.[20] All heterobimetallic complexes were also characterized by $^{195}Pt\{^1H\}$ NMR spectroscopy showing no changes with respect to the corresponding Pt(II) complexes as we already noticed in the case of heterobimetallic Pt(II)/Re(I) complexes.[9] HR-MS and elemental analyses of the various heterobimetallic complexes were in good agreement with the proposed structures.

Solid state structure

Single crystals suitable for X-Ray diffraction analysis of complex **3c** have been grown by slow diffusion of pentane into a saturated solution of **3c** in dichloromethane at 4 °C. The crystal structure of **3c** is depicted in figure 2.

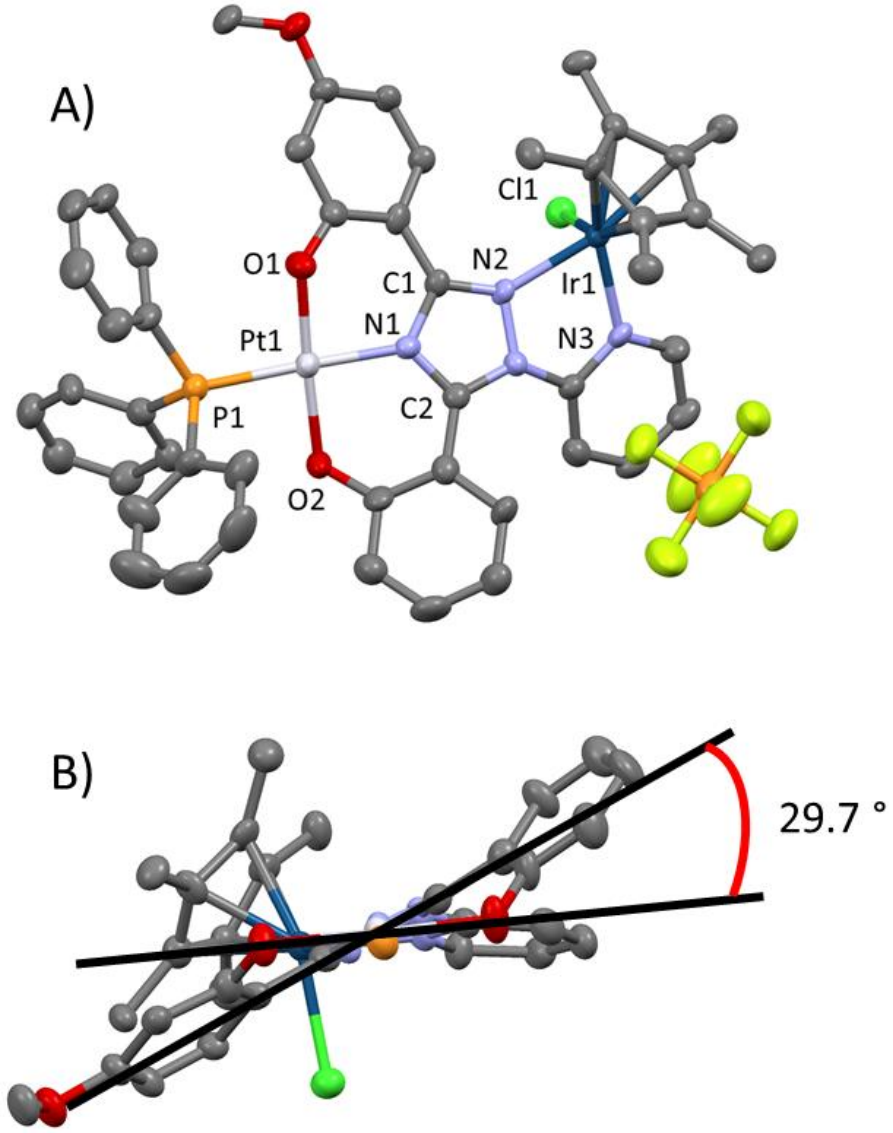

Figure 2: A) Crystal structure of complex **3c**. Ellipsoids set at 50% probability. Hydrogen atoms and solvent molecules have been omitted for clarity. Selected bond distances [Å] and angles [°] measured at 140 K: O_1-Pt_1 2.000(8), N_1-Pt_1 2.001(8), O_2-Pt_1 2.004(8), P_1-Pt_1 2.240(3), Ir_1-N_2 2.119(8), Ir_1-N_3 2.095(9), Ir_1-Cl_1 2.396(3), Ir_1-Cp* 1.787(10), O_1-Pt_1-N_1 88.7(3), O_1-Pt_1-P_1 93.3(2), O_2-Pt_1-N_1 88.9(3), O_2-Pt_1-P_1 89.2(2), O_1-Pt_1-O_2 176.9(3), N_1-Pt_1-P_1 178.0(2), N_2-Ir_1-N_3 75.2(3), N_3-Ir_1-Cl_1 83.8(3), N_2-Ir_1-Cl_1 86.9(2), N_2-Ir_1-Cp* 133.0(4), N_3-Ir_1-Cp* 132.3(4), Cl_1-Ir_1-Cp* 127.0(4). B) Visualization of the (O1-C1-C2-O2) torsion angle measured with Diamond software.[21]

As we already observed for heterobimetallic Pt(II)/Re(I) complexes, the Pt(II) cation adopts the typical slightly distorted square-planar geometry.[9] In the same way, the Ir(III) adopts a slightly distorted 6-coordinated « piano stool » geometry typical of Ir(III)-Cp* complexes.[22] Thus, in order to accommodate the first coordination sphere of both metals, the (O^N^O) pincer ligand is forced to adopt a distorted geometry characterized by a (O1-C1-C2-O2)

torsion angle of 29.7(6)° (figure 2B). This value being in between those of the neutral Pt(II)/Re(I) and that of the cationic Pt(II)/Re(I) complexes[9] it demonstrates that the $[(Cp^*)IrCl]^+$ fragment creates a steric hindrance between the $[BrRe(CO)_3]^+$ and the $[(pyridine)Re(CO)_3]^+$ fragments.

Stability study

We previously demonstrated the excellent stability of the Pt(II) complexes **1a-d** in aqueous environment.[9] In order to assess the outcome of the bimetallic complexes in aqueous conditions, all complexes **2a-d**, **3c-d** and **4c** were incubated at a concentration of 10^{-5} M in a DMSO/PBS (1:9) mixture up to 96 h at 37 °C and the corresponding UV-vis spectra were recorded at t = 0, 1 h, 24 h, 48 h, 72 h and 96 h (figure 3 and S1-5).

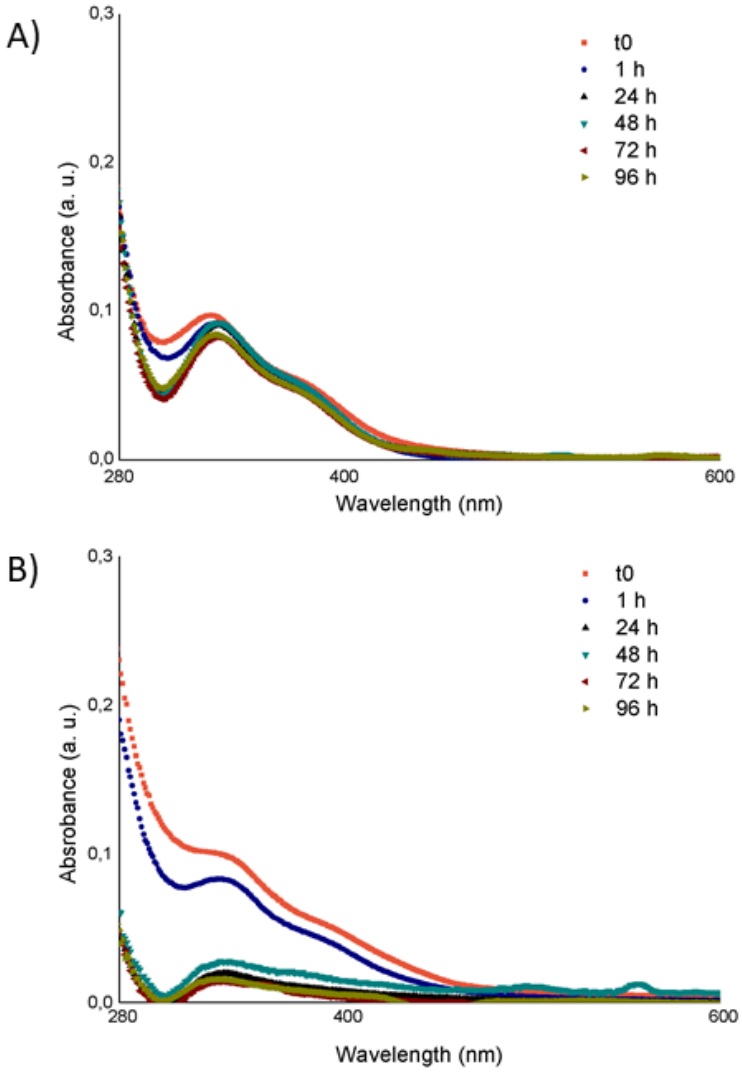

Figure 3: UV-Vis spectra recorded after incubation at a concentration of 10^{-5} M in PBS/DMSO 9:1 at 37 °C at t = 0, 1 h, 24 h, 48 h, 72 and 96 h for A) complex **2a** and B) complex **2b**.

From these spectra, we can distinguish two different behaviors according to the L ligand on the platinum center. For complexes bearing the DMSO (**2a**; figure 3A) and PPh_3 ligands (**2c**; figure S1, **3c**; figure S3 and **4c**; figure S5) no particular changes could be observed on the spectra over the 96 h of the study indicative that these bimetallic complexes did not undergo hydrolysis in this period of time. On the other hand, for complexes bearing a pyridine ligand (**2b**; figure 2B) and an NHC ligand (**2d**; figure S2 and **3d**; figure S4) a huge decrease of the absorbance between 280 and 420 nm is observed within the first 24 h of incubation. Considering that aquation of cationic [(arene)Ru(N^N)Cl]+ complexes, takes place within the first minutes after dissolution into aqueous medium,[23] we postulate that the drop of absorbance observed for complexes **2b**, **2d** and **3d** between 1 h and 24 h after the dissolution may be due to the decomposition of the [(arene)Ru(N^N)Cl]+ rather than to its aquation.

Partition coefficient determination

In the case of Pt(II)/Re(I) heterobimetallic complexes, we demonstrated that there was a relationship between the partition coefficient values (log $P_{o/w}$) and the intracellular uptake, with an optimum uptake for a log $P_{o/W}$ between 5 and 6.[9] Thus, for all Pt(II)/Ru(II), Pt(II)/Ir(III) and Pt(II)/Cu(I) complexes, the log $P_{o/w}$ values were measured using a well-established chromatographic method.[24] The results are reported in table 1.

Table 1: Log $P_{o/w}$ values measured by HPLC

Complex	Log $P_{o/W}$
1a[a]	3.67
1b[a]	3.34
1c[a]	6.86
1d[a]	4.50
2a	1.52
2b	3.15
2c	5.92
2d	3.02
3c	6.64
3d	2.96
4c	1.15

As one could have expected, both Pt(II)/Ru(II) and Pt(II)/Ir(III) complexes present lower log $P_{o/w}$ values than their Pt(II) precursors due to the addition of a cationic fragment on the molecular scaffold. Moreover, for a same monodentate ligand (either PPh_3 or NHC), both the

Pt(II)/(Ru(II) and Pt(II)/Ir(III) have very similar log $P_{o/w}$ values which can be explained by very similar structures of the added moiety ($(C_{10}H_{14})RuCl$ and $(C_{10}H_{15})IrCl$ respectively). Interestingly, the addition of the $[Cu(NHC)]^+$ moiety enhanced the hydrophilicity with respect to the Pt(II) precursor **1c**, as was observed for cationic Pt(II)/Re(I) complexes.[9]

In vitro antiproliferative activity

Although the complexes proved to be only poorly soluble in purely aqueous media, all compounds are soluble enough in DMSO not to precipitate when diluted in aqueous solution up to 100 µM with 1% DMSO. An initial screening of compounds **2a-d**, **3c-d** and **4c** was carried out on MDA-MB-231 « triple negative » human breast cancer cells. This cell line was chosen because platinum salts are currently the standard of care for this type of cancer although with variable outcome.[25] The inhibition of the proliferation of MDA-MB-231 cells was determined using the established MTT assay (see the experimental part for details) after 72 h of incubation with compounds **2a-d**, **3c-d** and **4c** and cisplatin at concentrations of 10 µM and 1 µM (figure 4).

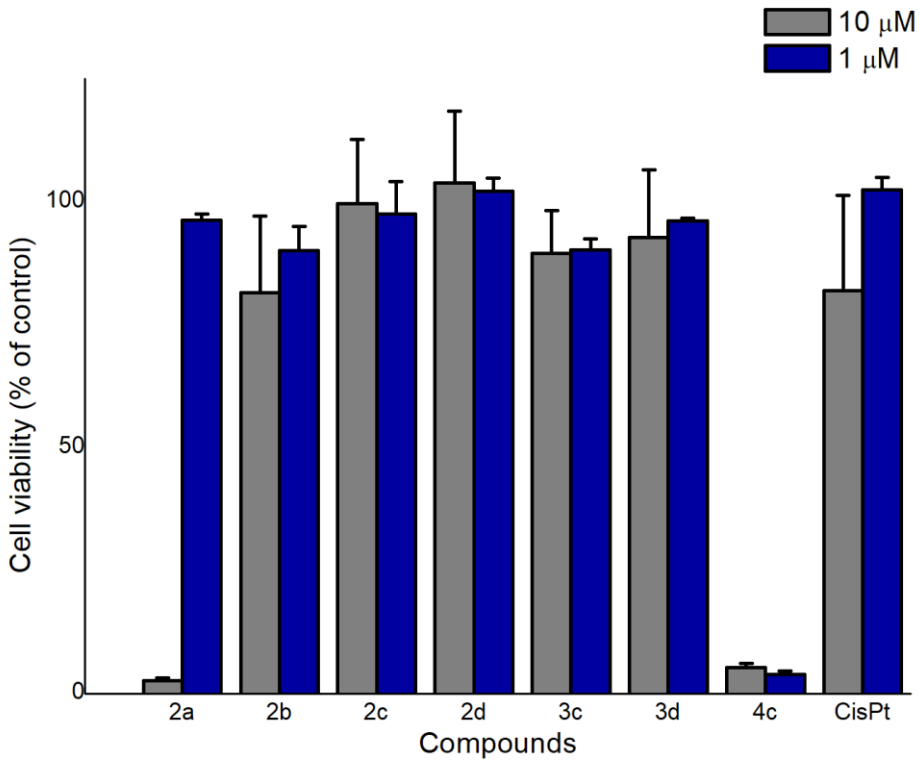

Figure 4: Inhibition of MDA-MB-231 cell growth by compounds **2a-d**, **3c-d** and **4c** and cisplatin; data represent the average ± standard error of three experiments.

Based on this screening we could identified two complexes as the most promising **2a** with an activity between 1 and 10 µM and **4c** with an activity below 1 µM. Considering the stability studies showing the degradation of the bimetallic complexes **2b**, **2d** and **3d** to lead to the corresponding non-toxic Pt(II) complexes,[9] it is not surprising that these complexes did not show any cytotoxicity at both concentrations. Thus, complexes **2a** and **4c** were selected for the measurement of their IC_{50} (concentration leading to a 50 % inhibition of cell growth) against a broader panel of human cancer cell lines including MDA-MB-231, MCF-7 (breast) and A2780 (ovary) as well as complexes **1a** and [(1,3(2,6(^{i}Pr)$_2$(C_6H_3))$_2$Im)CuCl] (**[(NHC^{iPr})CuCl]**) for comparison. To explore their potential selectivity, the compounds were also tested against the non-cancerous breast cells MCF-10A as comparison with respect to the breast cancer cells MDA-MB-231 and MCF-7 and considering their reported sensitivity to cisplatin.[26] Results are presented in table 2.

Table 2: Effect of compounds **1a**, **2a**, **4c**, **[(NHC^{iPr})CuCl]** and **cisplatin** on cell viability of a panel of human cancerous and non-cancerous cell lines after 72 h of incubation at 37 °C; data represent the average ± standard error of three experiments.

Complex	IC_{50} (µM)			
	MDA-MB-231	MCF-7	A2780	MCF-10A
1a[9]	3.1 ± 0.5	1.6 ± 0.9	1.5 ± 0.6	1.1 ± 0.2
2a	2.6 ± 0.4	4.1 ± 0.9	3.7 ± 0.9	2.9 ± 0.8
4c	0.16 ± 0.05	0.05 ± 0.02	0.05 ± 0.01	0.38 ± 0.08
[(NHC^{iPr})CuCl]	0.17 ± 0.04	0.04 ± 0.02	0.094 ± 0.007	0.8 ± 0.1
Cisplatin[9]	20.4 ± 3.4	14 ± 3.5	1.0 ± 0.2	2.9 ± 0.8

Complex **2a** appeared more toxic than Cisplatin on both breast cancer cell lines with activities 7.8 and 3.4 times higher than Cisplatin on MDA-MB-231 and MCF-7 cells respectively while complex **2a** demonstrated a reduced activity on A2780 cells with respect to Cisplatin. Moreover, it is worth noting that with the exception of MDA-MB-231 cells, complex **2a** appeared slightly less toxic than its Pt(II) precursor **1a** meaning that the cytotoxic properties of **2a** may come mainly from the Pt(II) moiety and that the incorporation of the [(*p*-cymene)RuCl]$^+$ moiety into the (N^N) chelate of **1a** had a deleterious impact on the cytotoxic properties of **1a** as was already observed in the case of Au(I)/Ru(II) heterobimetallic complexes.[19] Complex **4c** appeared more toxic than Cisplatin on every cancer cell lines being between 20 and 280 times more active than Cisplatin. Contrarily to what was observed for **2a**, the cytotoxic properties of **4c** seem to arise mainly from the [(NHC^{iPr})Cu]$^+$ moiety according to the IC_{50} values of complex **[(NHC^{iPr})CuCl]** that are in the submicromolar range for all tested cancer cell lines. These values are in good agreement with those already reported for similar Cu(I) complexes.[18] Moreover, when tested against non-cancerous breast cells MCF-10A, our heterobimetallic complexes demonstrated the same behavior than against the cancer cells. Indeed, Pt(II)/Ru(II) complex **2a** showed similar activity against MCF-10A cells (IC_{50} = 2.9 ± 0.8 µM) than against the cancer cells as was

already observed for its Pt(II) precursor **1a**. Pt(II)/Cu(I) complex **4c** showed interesting selectivities with IC_{50} value against the non-cancerous cells cells (IC_{50} = 0.38 ± 0.08 µM) being between 2 and 7.5 fold higher than the IC_{50} values against the different cancer cells. However, these selectivities are lower than those of the Cu(I) complex **[(NHC^{iPr})CuCl]** which appeared between 4.7 and 20 fold more active against the cancer cells than the non-cancerous cell line.

Conclusions

We have synthesized a series of seven new heterobimetallic complexes based on the [(O^N^O)Pt(L)] scaffold coupled to [(*p*-cymene)RuCl]$^+$, [(Cp*)IrCl]$^+$ or [(NHC^{iPr})Cu]$^+$ fragments with high yields. The complexes were characterized by various spectroscopic techniques including ^{1}H, ^{13}C{^{1}H} and ^{195}Pt{^{1}H} NMR spectroscopy and for complex **3c** by X-ray diffraction. That structure revealed the same distortion of the central (N^N)/(O^N^O) ligand that we already observed for Pt(II)/Re(I) complexes[9] in order to accommodate the coordination spheres of both the Pt(II) and the Ir(III) ions. All heterobimetallic complexes were screened for their antiproliferative activity against "triple negative" breast cancer cell line MDA-MB-231 enabling the identification of **2a** and **4c** as the most promising candidates. Although the compounds appeared more toxic than Cisplatin on the panel of tested human cancer cells, no positive combining effects could be observed from the tested heterobimetallic combinations. Similar results were obtained in terms of selectivity where the Cu(I) complex **[(NHC^{iPr})CuCl]** appeared the most selective for cancer cells, being up to 20 times more active on cancer cells than against the non-cancerous cell line.

Overall, this study demonstrated the great synthetic potential of this platform ligand for the efficient synthesis of heterobimetallic complexes which offers the possibility to explore various metal combinations for anti-cancer purposes.

Experimental part

General remarks

All reactions and manipulations were carried out under an argon atmosphere using standard Schlenk techniques. Anhydrous solvents were obtained by standard procedures. Chemicals were purchased from various manufacturers and used as received.^{1}H, ^{13}C, ^{31}P and ^{195}Pt NMR spectra were acquired on a Bruker 400 MHz spectrometer. Chemical shifts (δ) are expressed as ppm referenced to the solvent residual signal. Splitting patterns are expressed as follows: s, singlet; d, doublet; t, triplet; m, multiplet. Mass spectrometry was carried out at the HRMS facility of Sorbonne Université (Paris). High resolution mass spectra (HR-MS) were recorded on a LTQ-Orbitrap XL mass spectrometer (Thermo Scientific, San Jose, CA, USA) IR spectra were recorded on a Tensor 27 FT-IR spectrometer (Bruker). Elemental analysis was

performed at the elemental analysis service of ICSN (Gif-sur-Yvette, France). Complexes **1a-d** and **[(NHC^{iPr})CuCl]** have been synthesized according to reported procedures.[9,27]

Synthesis

Synthesis of **[Cl(*p*-cymene)Ru(L2)Pt(DMSO)]PF_6** (**2a**)

In a round-bottom flask **1a** (50 mg, 0.079 mmol) and **[Ru(*p*-cymene)Cl_2]$_2$** (24 mg, 0.040 mmol) and **KPF_6** (44 mg, 0.237 mmol) are dissolved in acetone (10 mL). The reaction mixture was stirred at room temperature overnight. Acetone was evaporated under reduced pressure and the product was dissolved in DCM. The suspension obtained was filtrated through a pad of celite, the filtrate concentrated under vacuum and upon addition of diethyl ether the product precipitated which lead after drying under vacuum to the pure product as an orange powder (66 mg, 0.063 mmol, 80 % yield). ^{1}H NMR ($CDCl_3$, 400 MHz, 298 K): δ 8.98 (d, $^3J_{H\text{-}H}$ = 5.2 Hz, 1 H, H^{19}), 8.91 (d, $^3J_{H\text{-}H}$ = 8.9 Hz, 1 H, H^5), 7.95 (t, $^3J_{H\text{-}H}$ = 7.6 Hz, 1 H, H^{17}), 7.76 (d, $^3J_{H\text{-}H}$ = 7.5 Hz, 1 H, H^{10}), 7.62 (m, 2 H, H^{16} + H^{18}), 7.41 (ddd, $^3J_{H\text{-}H}$ = 8.6 Hz, $^3J_{H\text{-}H}$ = 7.2 Hz, $^4J_{H\text{-}H}$ = 1.4 Hz, 1 H, H^{12}), 7.10 (d, $^3J_{H\text{-}H}$ = 8.4 Hz, 1 H, H^{13}), 6.88 (t, $^3J_{H\text{-}H}$ = 7.4 Hz, 1 H, H^{11}), 6.54 (m, 2 H, H^2 +H^4), 5.95 (m, 2 H, H^{21} + H^{22}), 5.52 (m, 2 H, H^{21} + H^{22}), 3.87 (s, 3 H, OMe), 3.45 (s, 3 H, S(O)Me), 3.41 (s, 3 H, S(O)Me), 2.75 (h, $^3J_{H\text{-}H}$ = 6.9 Hz, 1 H, CH_{iPr}), 2.16 (s, 3 H, Me_{Ar}), 1.22 (m, 6 H, Me_{iPr}). ^{13}C{^{1}H} Jmod NMR ($CDCl_3$, 100 MHz, 298 K): δ 168.9 (s, *C*^{14}), 168.7 (s, *C*^{1}), 165.3 (s, *C*^{3}), 157.4 (s, *C*^{6}), 155.6 (s, *C*^{19}), 148.3 (s, *C*^{9}), 147.4 (s, *C*^{15}), 141.2 (s, *C*^{17}), 136.6 (s, *C*^{12}), 131.1 (s, *C*^{5}), 129.1 (s, *C*^{10}), 126.5 (s, *C*^{18}), 124.1 (s, *C*^{13}), 118.5 (s, *C*^{11}), 115.3 (s, *C*^{16}), 108.5 (s, *C*^{21}), 108.1 (s, *C*^{8}), 107.9 (s, *C*^{4}), 104.0 (s, *C*^{2}), 102.1 (s, *C*^{7}), 100.6 (s, *C*^{20}), 86.1 (s, *C*^{21}), 85.8 (s, *C*^{21}), 83.8 (s, *C*^{22}), 82.6 (s, *C*^{22}), 55.7 (s, O*C*H_3), 41.2 (s, S(O)*C*H_3), 40.6 (s, S(O)*C*H_3), 31.3 (s, *C*H_{iPr}), 21.1 (s, *C*$H_{3\text{-}iPr}$), 22.0 (s, *C*$H_{3\text{-}iPr}$), 18.4 (s, *C*$H_{3\text{-}Ar}$). ^{195}Pt{^{1}H} NMR ($CDCl_3$, 86 MHz, 298 K): δ -2318 (s, Cl(*p*-cymene)Ru(L2)*Pt*(DMSO)). ESI-MS (MeCN) *positive mode exact mass* for $[C_{32}H_{34}N_4O_4SClPtRu]^+$ (902.0681): measured *m/z* 902.0684 $[M\text{-}PF_6]^+$. Calcd for $C_{32}H_{34}N_4O_4SPtRuClPF_6$ (1047.3): C, 36.70; H, 3.27; N, 5.35; S, 3.06. Found: C, 36.95; H, 3.28; N, 5.37; S, 2.81. IR υ_{max} (neat/cm^{-1}): 1148 (S=O).

Synthesis of **[Cl(*p*-cymene)Ru(L2)Pt(pyridine)]PF_6** (**2b**)

In a round-bottom flask **1b** (50 mg, 0.079 mmol) and **[Ru(*p*-cymene)Cl_2]$_2$** (24 mg, 0.040 mmol) and **KPF_6** (44 mg, 0.237 mmol) were dissolved in acetone (10 mL). The reaction was performed at room temperature overnight. Acetone was evaporated under reduced pressure and the product was dissolved in DCM. The obtained solution was filtrated through a pad of celite, concentrated under vacuum and upon addition of cyclohexane the product precipitated which led after drying under vacuum to the pure product as an orange powder (60 mg, 0.058 mmol, 73 % yield). ^{1}H NMR ($CDCl_3$, 400 MHz, 298 K): δ 8.95 (m, 4 H, H^5 + H^{19} + H^{20}), 8.01 (t, $^3J_{H\text{-}H}$ = 7.4 Hz, 1 H, H^{22}), 7.92 (t, $^3J_{H\text{-}H}$ = 8.0 Hz, 1 H, H^{17}), 7.68 (d, $^3J_{H\text{-}H}$ = 7.6 Hz, 1

H, H^{10}), 7.55-7.61 (m, 4 H, H^{16} + H^{18} + H^{21}), 7.39 (t, $^3J_{H-H}$ = 6.2 Hz, 1 H, H^{12}), 7.13 (d, $^3J_{H-H}$ = 8.1 Hz, 1 H, H^{13}), 6.82 (t, $^3J_{H-H}$ = 7.2 Hz, 1 H, H^{11}), 6.58 (s, 1 H, H^2), 6.50 (d, $^3J_{H-H}$ = 9.3 Hz, 1 H, H^4), 5.91 (m, 2 H, H^{24} + H^{25}), 5.53 (m, 2 H, H^{24} + H^{25}), 3.88 (s, 3 H, OMe), 2.74 (h, $^3J_{H-H}$ = 6.7 Hz, 1 H, CH_{iPr}), 2.19 (s, 3 H, Me_{Ar}), 1.21 (t, $^3J_{H-H}$ = 6.7 Hz, 6 H, Me_{iPr}). $^{13}C\{^1H\}$ Jmod NMR ($CDCl_3$, 100 MHz, 298 K): δ 169.2 (s, $C^{1/14}$), 169.1 (s, $C^{1/14}$), 164.9 (s, C^3), 157.8 (s, C^6), 155.6 (s, C^{19}), 148.9 (s, C^{20}), 147.9 (s, C^9), 147.6 (s, C^{15}), 141.0 (s, C^{17}), 139.2 (s, C^{22}), 135.9 (s, C^{12}), 131.3 (s, C^5), 129.0 (s, C^{10}), 126.1 (s, C^{18}), 125.4 (s, C^{21}), 123.9 (s, C^{13}), 118.1 (s, C^{11}), 115.1 (s, C^{16}), 108.6 (s, C^8), 108.3 (s, C^{26}), 107.4 (s, C^4), 103.7 (s, C^2), 102.3 (s, C^7), 100.1 (s, C^{23}), 86.2 (s, C^{25}), 86.0 (s, C^{25}), 83.7 (s, C^{24}), 82.6 (s, C^{24}), 55.6 (s, OCH_3), 31.4 (s, CH_{iPr}), 22.0 (s, $CH_{3\text{-}iPr}$), 18.4 (s, $CH_{3\text{-}Ar}$). $^{195}Pt\{^1H\}$ NMR ($CDCl_3$, 86 MHz, 298 K): δ -1541. ESI-MS (MeCN) *positive mode exact mass* for $[C_{35}H_{33}N_5O_3ClPtRu]^+$ (903.0958): measured *m/z* 903.0971 $[M\text{-}PF_6]^+$. Calcd for $C_{35}H_{33}N_5O_3PtRuClPF_6$ (1048.2): C, 40.10; H, 3.17; N, 6.68. Found: C, 40.17; H, 3.41; N, 6.53.

Synthesis of **[Cl(*p*-cymene)Ru(L2)Pt(PPh_3)]PF_6** (**2c**)

In a round-bottom flask **1c** (50 mg, 0.061 mmol) and **[Ru(*p*-cymene)Cl_2]$_2$** (19 mg, 0.031 mmol) and **KPF_6** (34 mg, 0.183 mmol) were dissolved in acetone (5 mL). The reaction was performed at room temperature overnight. Acetone was evaporated under reduced pressure and the product was dissolved in DCM. The obtained solution was filtrated through a pad of celite, concentrated under vacuum and upon addition of cyclohexane the product precipitated which led after drying under vacuum to the pure product as an orange powder (66 mg, 0.053 mmol, 87 % yield). ^1H NMR ($CDCl_3$, 400 MHz, 298 K): δ 9.00 (dd, $^3J_{H-H}$ = 5.7 Hz, $^4J_{H-H}$ = 0.8 Hz, 1 H, H^{19}), 8.90 (d, $^3J_{H-H}$ = 9.1 Hz, 1 H, H^5), 7.91 (ddd, $^3J_{H-H}$ = 9.5 Hz, $^3J_{H-H}$ = 8.3 Hz, $^4J_{H-H}$ = 1.6 Hz, 1 H, H^{17}), 7.73-7.78 (m, 6 H, H^{22}), 7.69 (dd, $^3J_{H-H}$ = 8.3 Hz, $^4J_{H-H}$ = 1.6 Hz, 1 H, H^{10}), 7.54-7.62 (m, 5 H, H^{16} + H^{18} + H^{23}), 7.46-7.51 (m, 6 H, H^{21}), 7.26 (m, 1 H, H^{12}), 6.82 (ddd, $^3J_{H-H}$ = 8.1 Hz, $^3J_{H-H}$ = 6.8 Hz, $^4J_{H-H}$ = 1.0 Hz, 1 H, H^{11}), 6.53 (dd, $^3J_{H-H}$ = 8.7 Hz, $^4J_{H-H}$ = 0.9 Hz, 1 H, H^{13}), 6.45 (dd, $^3J_{H-H}$ = 9.1 Hz, $^4J_{H-H}$ = 2.6 Hz, 1 H, H^4), 5.95 (d, $^4J_{H-H}$ = 2.5 Hz, 1 H, H^2), 5.91 (t, $^3J_{H-H}$ = 6.0 Hz, 2 H, H^{26}), 5.52 (d, $^3J_{H-H}$ = 5.5 Hz, 2 H, H^{25}), 3.73 (s, 3 H, OMe), 2.79 (h, $^3J_{H-H}$ = 6.9 Hz, 1 H, CH_{iPr}), 2.17 (s, 3 H, Me_{Ar}), 1.24 (d, $^3J_{H-H}$ = 6.8 Hz, 3 H, Me_{iPr}), 1.22 (d, $^3J_{H-H}$ = 6.8 Hz, 3 H, Me_{iPr}). $^{13}C\{^1H\}$ Jmod NMR ($CDCl_3$, 100 MHz, 298 K): δ 169.7 (s, $C^{1/14}$), 169.6 (s, $C^{1/14}$), 164.7 (s, C^3), 158.2 (s, C^6), 155.7 (s, C^{19}), 148.7 (s, C^9), 147.6 (s, C^{15}), 141.0 (s, C^{17}), 135.9 (s, C^{12}), 134.6 (d, $^3J_{P-C}$ = 11.1 Hz, C^{22}), 131.4 (d, $^4J_{P-C}$ = 2.5 Hz, C^{23}), 131.1 (s, C^5), 129.1 (s, C^{10}), 128.6 (d, $^2J_{P-C}$ = 11.2 Hz, C^{21}), 127.4 (d, $^1J_{P-C}$ = 62.4 Hz, C^{20}), 126.1 (s, C^{18}), 124.6 (s, C^{13}), 117.9 (s, C^{11}), 114.8 (s, C^{16}), 109.2 (s, C^8), 108.5 (s, C^{27}), 107.1 (s, C^4), 104.5 (s, C^2), 103.1 (s, C^7), 100.7 (s, C^{24}), 86.0 (s, C^{25}), 85.8(s, C^{26}), 84.0(s, C^{26}), 82.5 (s, C^{25}), 55.3 (s, OCH_3), 31.3 (s, CH_{iPr}), 22.2 (s, $CH_{3\text{-}iPr}$), 22.0 (s, $CH_{3\text{-}iPr}$), 18.5 (s, $CH_{3\text{-}Ar}$). $^{31}P\{^1H\}$ NMR ($CDCl_3$, 162 MHz, 298 K): δ 8.35 (t, $^1J_{P-Pt}$ = 4281 Hz, 1 P, PPh_3), -144.5 (h, $^1J_{P-F}$ = 713 Hz, 1 P, PF_6). $^{195}Pt\{^1H\}$ NMR ($CDCl_3$, 86 MHz, 298 K): δ -2452 (d, $^1J_{P-Pt}$ = 4303 Hz, Cl(*p*-cymene)Ru(L2)*Pt*(PPh_3)). ESI-MS (MeCN) *positive mode exact mass* for $[C_{48}H_{43}N_4O_3PClPtRu]^+$ (1086.1447): measured *m/z* 1086.1464 $[M\text{-}PF_6]^+$. Calcd for $C_{48}H_{43}N_4O_3PPtRuClPF_6$ (1231.1): C, 46.82; H, 3.52; N, 4.55. Found: C, 46.91; H 3.54; N 4.27.

Synthesis of **[Cl(*p*-cymene)Ru(L2)Pt(1,3-dimethylbenzimidazol-2-ylidene)]PF_6** (**1d**)

In a round-bottom flask **1d** (40 mg, 0.057 mmol) and **[Ru(*p*-cymene)Cl_2]$_2$** (18 mg, 0.029 mmol) and **KPF_6** (32 mg, 0.172 mmol) were dissolved in acetone (5 mL). The reaction was performed at room temperature overnight. Acetone was evaporated under reduced pressure and the product was dissolved in DCM. The obtained solution was filtrated through a pad of celite, concentrated under vacuum and upon addition of diethyl ether the product precipitated which led after drying under vacuum to the pure product as an orange powder (55 mg, 0.049 mmol, 86 % yield). ^{1}H NMR ($CDCl_3$, 400 MHz, 298 K): δ 9.03 (m, 2 H, H^5 + H^{19}), 7.93 (t, $^3J_{H-H}$ = 8.0 Hz, 1 H, H^{17}), 7.75 (dd, $^3J_{H-H}$ = 8.2 Hz, $^4J_{H-H}$ = 1.4 Hz, 1 H, H^{16}), 7.61 (m, 2 H, H^{10} + H^{18}), 7.50 (m, 2 H, H^{22}), 7.41 (m, 3 H, H^{12} + H^{23}), 7.02 (dd, $^3J_{H-H}$ = 8.8 Hz, $^4J_{H-H}$ = 0.9 Hz, 1 H, H^{13}), 6.86 (ddd, $^3J_{H-H}$ = 8.2 Hz, $^3J_{H-H}$ = 7.0 Hz, $^4J_{H-H}$ = 1.1 Hz, 1 H, H^{11}), 6.53 (dd, $^3J_{H-H}$ = 9.1 Hz, $^4J_{H-H}$ = 2.5 Hz, 1 H, H^4), 6.45 (d, $^4J_{H-H}$ = 2.5 Hz, 1 H, H^2), 5.95 (m, 2 H, H^{25} + H^{26}), 5.57 (m, 2 H, H^{25} + H^{26}), 4.27 (s, 6 H, NMe), 3.83 (s, 3 H, OMe), 2.82 (h, $^3J_{H-H}$ = 6.9 Hz, 1 H, CH_{iPr}), 2.21 (s, 3 H, $CH_{3\text{-}Ar}$), 1.25 (d, $^3J_{H-H}$ = 6.9 Hz, 6 H, $CH_{3\text{-}iPr}$). ^{13}C{^{1}H} Jmod NMR ($CDCl_3$, 100 MHz, 298 K): δ 169.4 (s, $C^{1/14}$), 169.3 (s, $C^{1/14}$), 164.9 (s, C^3), 160.7 (s, C^{20}), 158.1 (s, C^6), 155.7 (s, C^{19}), 148.3 (s, C^9), 147.6 (s, C^{15}), 141.1 (s, C^{17}), 135.9 (s, C^{12}), 134.9 (s, C^{21}), 131.4 (s, C^5), 129.2 (s, C^{16}), 126.0 (s, C^{10}), 124.0 (s, C^{23}), 123.9 (s, C^{13}), 117.8 (s, C^{11}), 114.9 (s, C^{18}), 110.5 (s, C^{22}), 109.0 (s, C^8), 108.3 (s, C^{27}), 106.8 (s, C^4), 103.9 (s, C^2), 103.0 (s, C^7), 100.9 (s, C^{24}), 85.7 (s, C^{25}), 83.9 (s, C^{26}), 82.6 (s, C^{26}), 55.5 (s, OCH_3), 33.8 (s, NCH_3), 31.3 (s, CH_{iPr}), 22.2 (s, $CH_{3\text{-}iPr}$), 21.9 (s, $CH_{3\text{-}iPr}$), 18.5 (s, $CH_{3\text{-}Ar}$). ^{195}Pt{^{1}H} NMR ($CDCl_3$, 86 MHz, 298 K): δ -2110 (s, Cl(*p*-cymene)Ru(L2)*Pt*(NHC)). ESI-MS (MeCN) *positive mode exact mass* for $[C_{39}H_{38}N_6O_3ClPtRu]^+$ (970.1380): measured *m/z* 970.1397 $[M\text{-}PF_6]^+$. Calcd for $C_{39}H_{38}N_6O_3ClPtRuPF_6.H_2O$ (1133.4): C, 41.33; H, 3.56; N, 7.42. Found: C, 41.21; H 3.38; N 7.41.

Synthesis of **[Cl(Cp*)Ir(L2)Pt(PPh_3)]PF_6** (**3c**)

In a round-bottom flask **1c** (50 mg, 0.061 mmol) and **[Ir(Cp*)Cl_2]$_2$** (25 mg, 0.031 mmol) and **KPF_6** (34 mg, 0.183 mmol) are dissolved in acetone (5 mL). The reaction was at room temperature overnight. Acetone was evaporated under reduced pressure and the product was dissolved in DCM. The obtained solution was filtrated through a pad of celite, concentrated under vacuum and upon addition of diethyl ether the product precipitated which lead after filtration and drying under vacuum to the pure product as an orange powder (68 mg, 0.051 mmol, 84 % yield). ^{1}H NMR (CD_3CN, 400 MHz, 298 K): δ 8.77 (d, $^3J_{H-H}$ = 9.1 Hz, 1 H H^5), 8.68 (d, $^3J_{H-H}$ = 5.1 Hz, 1 H, H^{19}), 8.06 (t, $^3J_{H-H}$ = 8.1 Hz, 1 H, H^{17}), 7.76-7.80 (m, 6 H, H^{21}), 7.73 (d, $^3J_{H-H}$ = 8.5 Hz, 1 H, H^{16}), 7.60-7.67 (m, 5 H, H^{10} + H^{18} + H^{23}), 7.51-7.56 (m, 6 H, H^{22}), 7.33 (ddd, $^3J_{H-H}$ = 8.6 Hz, $^3J_{H-H}$ = 7.0 Hz, $^4J_{H-H}$ = 1.6 Hz, 1 H, H^{12}), 6.73 (ddd, $^3J_{H-H}$ = 8.1 Hz, $^3J_{H-H}$ = 7.0 Hz, $^4J_{H-H}$ = 0.9 Hz, 1 H, H^{11}), 6.61 (d, $^3J_{H-H}$ = 8.6 Hz, 1 H, H^{13}), 6.39 (dd, $^3J_{H-H}$ = 9.0 Hz, $^4J_{H-H}$ = 2.5 Hz, 1 H, H^4), 5.83 (d, $^4J_{H-H}$ = 2.5 Hz, 1 H, H^2), 3.67 (s, 3 H, OMe), 1.54 (s, 15 H,

Me_{Cp*}). $^{13}C\{^1H\}$ Jmod NMR (CD_3CN, 100 MHz, 298 K): δ 170.0 (s, C^{14}), 169.8 (s, C^1), 165.7 (s, C^3), 155.1 (s, C^6), 153.2 (s, C^{19}), 150.8 (s, C^9), 148.9 (s, C^{15}), 142.8 (s, C^{17}), 136.6 (s, C^{12}), 135.3 (d, $^3J_{P-C}$ = 11.7 Hz, C^{22}), 132.5 (d, $^4J_{P-C}$ = 3.5 Hz, C^{23}), 132.1 (s, C^5), 130.6 (s, C^{10}), 129.6 (d, $^2J_{P-C}$ = 11.1 Hz, C^{21}), 128.4 (d, $^1J_{P-C}$ = 62.3 Hz, C^{20}), 127.4 (s, C^{18}), 124.9 (s, C^{13}), 117.9 (s, C^{11}), 116.5 (s, C^{16}), 110.4 (s, C^8), 108.1 (s, C^4), 104.7 (s, C^2), 104.3 (s, C^7), 90.7 (s, C^{24}), 56.0 (s, OCH_3), 9.0 (s, CH_{3-Cp*}). $^{31}P\{^1H\}$ NMR (CD_3CN, 162 MHz, 298 K): δ 8.53 (t, $^1J_{P-Pt}$ = 4245 Hz, 1 P, PPh_3), -144.6 (h, $^1J_{P-F}$ = 707 Hz, 1 P, PF_6). $^{195}Pt\{^1H\}$ NMR (CD_3CN, 86 MHz, 298 K): δ -2458 (d, $^1J_{P-Pt}$ = 4320 Hz, Cl(Cp*)Ir(L2)*Pt*(PPh_3)). ESI-MS (MeCN) *positive mode exact mass* for $[C_{48}H_{44}N_4O_3PClPtIr]^+$ (1178.2111): measured *m/z* 1178.2127 $[M\text{-}PF_6]^+$. Calcd for $C_{48}H_{44}N_4O_3PClPtIrPF_6.2H_2O$ (1323.6): C, 42.40; H, 3.56; N, 4.12. Found: C, 42.44; H 3.34; N 4.02.

Synthesis of **[Cl(Cp*)Ir(L2)Pt(1,3-dimethylbenzimidazol-2-ylidene)]PF_6** (**3d**)

In a round-bottom flask **1d** (40 mg, 0.057 mmol) and **$[Ir(Cp^*)Cl_2]_2$** (23 mg, 0.029 mmol) and **KPF_6** (32 mg, 0.172 mmol) are dissolved in acetone (5 mL). The reaction was at room temperature overnight. Acetone was evaporated under reduced pressure and the product was dissolved in DCM. The obtained solution was filtrated through a pad of celite, concentrated under vacuum and upon addition of diethylether the product precipitated which lead after filtration and drying under vacuum to the pure product as an orange powder (58 mg, 0.048 mmol, 84 % yield). ^1H NMR (CD_3CN, 400 MHz, 298 K): δ 8.86 (d, $^3J_{H-H}$ = 9.3 Hz, 1 H, H^5), 8.69 (dd, $^3J_{H-H}$ = 5.7 Hz, $^4J_{H-H}$ = 1.2 Hz, 1 H, H^{19}), 8.07 (ddd, $^3J_{H-H}$ = 8.8 Hz, $^3J_{H-H}$ = 7.6 Hz, $^4J_{H-H}$ = 1.5 Hz, 1 H, H^{17}), 7.72 (d, $^3J_{H-H}$ = 8.6 Hz, 1 H, H^{16}), 7.64-7.67 (m, 4 H, H^{10} + H^{18} + H^{21}), 7.41-7.47 (m, 3 H, H^{12} + H^{23}), 7.03 (d, $^3J_{H-H}$ = 8.0 Hz, 1 H, H^{13}), 6.72 (ddd, $^3J_{H-H}$ = 8.0 Hz, $^3J_{H-H}$ = 6.8 Hz, $^4J_{H-H}$ = 1.0 Hz, 1 H, H^{11}), 6.43-6.45 (m, 2 H, H^2 + H^4), 4.26 (s, 6 H, NMe), 3.78 (s, 3 H, OMe), 1.57 (s, 15 H, Me_{Cp*}). $^{13}C\{^1H\}$ Jmod NMR (CD_3CN, 100 MHz, 298 K): δ 170.2 (s, C^{14}), 170.0 (s, C^1), 165.8 (s, C^3), 162.0 (s, C^{20}), 155.1 (s, C^6), 153.2 (s, C^{19}), 150.5 (s, C^9), 149.0 (s, C^{15}), 142.7 (s, C^{17}), 136.3 (s, C^{12}), 135.4 (s, C^{21}), 132.3 (s, C^5), 130.6 (s, C^{10}), 127.2 (s, C^{18}), 124.8 (s, C^{23}), 124.7 (s, C^{13}), 117.6 (s, C^{11}), 116.5 (s, C^{16}), 111.9 (s, C^{22}), 110.2 (s, C^8), 107.5 (s, C^4), 104.6 (s, C^2), 104.1 (s, C^7), 90.6 (s, C^{24}), 56.1 (s, OCH_3), 34.3 (s, NCH_3), 9.1 (s, CH_{3-Cp*}). $^{195}Pt\{^1H\}$ NMR ($CDCl_3$, 86 MHz, 298 K): δ -2097 (s, Cl(Cp*)Ir(L2)*Pt*(NHC)). ESI-MS (MeCN) *positive mode exact mass* for $[C_{39}H_{39}N_6O_3ClPtIr]^+$ (1062.2044): measured *m/z* 1062.2062 $[M\text{-}PF_6]^+$. Calcd for $C_{39}H_{39}N_6O_3PtIrClPF_6$ (1207.5): C, 38.79; H, 3.26; N, 6.96. Found: C, 38.90; H 3.38; N 6.80.

Synthesis of **[(1,3(2,6(^{i}Pr)$_2$(C_6H_3))$_2$Im)Cu(L2)Pt(PPh_3)]BF_4** (**4c**)

In a round-bottom flask **(1,3(2,6(^{i}Pr)$_2$(C_6H_3))$_2$Im)CuCl** (30 mg, 0.061 mmol) was dissolved in 3 mL of DCM. **$AgBF_4$** (12 mg, 0.061 mmol) was dissolved in 2 mL of acetone and added to **(1,3(2,6(^{i}Pr)$_2$(C_6H_3))$_2$Im)CuCl** at room temperature leading to the formation of a white

precipitate. The reaction was kept 30 min at room temperature. **1c** (50 mg, 0.061 mmol) was dissolved in 5 mL of DCM and added on the previous mixture at room temperature. The reaction was kept overnight at room temperature. The reaction mixture was filtered through a pad of celite and the solvents were evaporated. Precipitation with pentane from a concentrated solution in DCM led to the formation of a yellow solid which gave after drying the pure product as a yellow powder (80 mg, 0.059 mmol, 97 % yield). ^{1}H NMR ($CDCl_3$, 400 MHz, 298 K): δ 8.43 (broad s, 1 H, H^{19}), 7.99 (dt, $^{3}J_{H-H}$ = 7.9 Hz, $^{4}J_{H-H}$ = 1.9 Hz, 1 H, H^{17}), 7.74-7.83 (m, 7 H, H^{5} + H^{22}), 7.41-7.62 (m, 14 H, H^{16} + H^{18} + H^{21} + H^{23} + H^{25} + H^{29}), 7.10-7.24 (m, 4 H, H^{28} + H^{30}), 7.04 (dt, $^{3}J_{H-H}$ = 6.9 Hz, $^{4}J_{H-H}$ = 1.5 Hz, 1 H, H^{12}), 6.83 (d, $^{3}J_{H-H}$ = 7.9 Hz, 1 H, H^{10}), 6.49 (d, $^{3}J_{H-H}$ = 7.9 Hz, 1 H, H^{13}), 6.38 (t, $^{3}J_{H-H}$ = 7.5 Hz, 1 H, H^{11}), 6.07 (d, $^{3}J_{H-H}$ = 8.8 Hz, 1 H, H^{4}), 5.90 (d, $^{4}J_{H-H}$ = 2.4 Hz, 1 H, H^{2}), 3.56 (s, 3 H, OMe), 2.57 (broad s, 2 H, CH_{iPr}), 2.40 (broad s, 2 H, CH_{iPr}), 1.20 (m, 18 H, Me_{iPr}), 1.03 (broad s, 6 H, Me_{iPr}). $^{13}C\{^{1}H\}$ Jmod NMR ($CDCl_3$, 100 MHz, 298 K): δ 166.7 (s, C^{14}), 165.2 (s, C^{1}), 162.3 (s, C^{3}), 152.6 (s, C^{6}), 150.6 (s, C^{15}), 149.8 (s, C^{19}), 146.5 (s, C^{9}), 145.5 (s, C^{27} + C^{31}), 145.3 (s, C^{24}), 140.2 (s, C^{17}), 134.7 (d, , $^{2}J_{P-C}$ = 10.1 Hz, C^{21}), 132.6 (s, C^{12}), 130.9 (d, , $^{4}J_{P-C}$ = 2.0 Hz, C^{23}), 130.8 (s, C^{25}), 128.4 (d, , $^{3}J_{P-C}$ = 11.5 Hz, C^{22}), 128.3 (d, , $^{1}J_{P-C}$ = 60.8 Hz, C^{20}), 128.2 (s, C^{5} + C^{10}), 125.6 (s, C^{29}), 124.4 (s, C^{18}), 124.3 (s, C^{28} + C^{30}), 123.6 (s, C^{13}), 120.0 (s, C^{16}), 115.8 (s, C^{11}), 110.3 (s, C^{8}), 105.8 (s, C^{7}), 105.7 (s, C^{4}), 104.1 (s, C^{2}), 55.0 (s, OCH_3), 28.8 (s, CH_{iPr}), 28.6 (s, CH_{iPr}), 24.7 (s, $CH_{3\text{-}iPr}$), 24.6 (s, $CH_{3\text{-}iPr}$), 24.0 (s, $CH_{3\text{-}iPr}$). $^{31}P\{^{1}H\}$ NMR ($CDCl_3$, 162 MHz, 298 K): δ 9.25 (t, $^{1}J_{P-Pt}$ = 4205 Hz, 1 P, PPh_3). $^{195}Pt\{^{1}H\}$ NMR ($CDCl_3$, 86 MHz, 298 K): δ -2410 (d, $^{1}J_{P-Pt}$ = 4232 Hz, (1,3(2,6(^{i}Pr)$_2$(C_6H_3))$_2$Im)Cu(L2)*Pt*(PPh_3)).ESI-MS (MeCN) *positive mode exact mass* for $[C_{65}H_{65}N_6O_3PPtCu]^+$ (1266.3794): measured *m/z* 1266.3799 $[M\text{-}BF_4]^+$. Calcd for $C_{65}H_{65}N_6O_3PPtCuBF_4$ (1354.7): C, 57.63; H, 4.84; N, 6.20. Found: C, 57.35; H 4.94; N 6.15.

X-Ray crystal structure determination

A single crystal was selected, mounted and transferred into a cold nitrogen gas stream. Intensity data was collected with a Bruker Kappa-APEX2 system using micro-source Cu-Kα radiation. Unit-cell parameters determination, data collection strategy, integration and absorption correction were carried out with the Bruker APEX2 suite of programs. The structure was solved with SHELXT and refined anisotropically by full-matrix least-squares methods with SHELXL using the WinGX suite. The crystal was refined as a two-component twin. The structure was deposited at the Cambridge Crystallographic Data Centre with number CCDC 2009121 and can be obtained free of charge via www.ccdc.cam.ac.uk.

Crystal data for **3c.** $C_{51}H_{50}Cl_7F_6IrN_4O_3P_2Pt$, triclinic P -1, a = 8.3896(9) Å, b = 16.9203(18) Å, c = 21.152(2) Å, α = 104.536(3)°, β = 96.991(4)°, γ = 95.511(4)°, V = 2859.7(5) Å^3, Z = 2, orange prism 0.3 × 0.15 × 0.1 mm^3, μ = 13.040 mm^{-1}, min / max transmission = 0.03 / 0.16, T= 140(1) K, λ = 1.54178 Å, θ range = 2.73° to 67.03°, 14614 reflections measured, R_{int} = 0.0788, completeness = 0.958, 682 parameters, 0 restraints, final R indices R1 [I>2σ(I)] = 0.0598 and wR2 (all data) = 0.1749, GOF on F^2 = 1.093, largest difference peak / hole = 2.87 / -1.84 e·Å^{-3}.

Log $P_{o/w}$ determination by HPLC

Solutions of different compounds were prepared at 1 mM in MeOH. To 200 µL of these solutions, 10 µL of uracil solution (5 mM in MeOH) were added as internal standard and solutions were further diluted to a final concentration of 250 µM. Measurement of the octanol/water partition coefficient (log $P_{o/w}$) was done by HPLC technique according to the method previously described.[23] Measurement of the chromatographic capacity factors (k) for each molecule was done by varying the percentage of organic eluent (methanol containing 0.25% 1-octanol (v/v)) in the 98–60% range in the aqueous eluent (0.15% n-decylamine (v/v) in MOPS buffer pH 7.4 prepared in 1-octanol saturated water). These capacity factors (k') were extrapolated to 100% of the aqueous eluent, giving the value of k'_w. The log $P_{o/w}$ was obtained by the formula: Log Po/w = 0.31418 + 0.98452 log k'_w.

Cell culture and cell growth inhibition

Human breast cancer cell lines MCF-7 and MDA-MB-231 (ATCC) were cultivated in DMEM (Dulbecco's Modified Eagle Medium) containing GlutaMaxI supplemented with 10% FBS (ThermoFisher Scientific) and 1% kanamycin at 37 °C in a humidified atmosphere and 5% CO_2. Human ovarian cancer cells A2780 (ATCC) were cultured in RPMI1640 containing GlutaMax I supplemented with 10% FBS (ThermoFisher Scientific) and 1% kanamycin at 37 °C in a humidified atmosphere and 5% CO_2. Non-cancerous cell line MCF-10A (ATCC) was maintained in DMEM:F12 (1:1) cell culture media, 5 % heat inactivated horse serum (ThermoFisher Scientific), supplemented with HEPES (20 mM), L-glutamine (2 mM), epidermal growth factor (20 ng/mL), hydrocortisone (500 ng/mL), cholera toxin (100 ng/mL), and insulin (10 µg/mL). Cell viability was evaluated by using a colorimetric method based on the tetrazolium salt MTT [3-(4,5- dimethylthiazol-2-yl)-2,5-diphenyltetrazolium bromide], which is reduced by viable cells to yield purple formazan crystals. Cells were seeded in 96-well plates at a density of 40000 cells/mL (100 µL per well). After overnight attachment, a dilution series of the compounds were added in the medium, and cells were incubated for a further 72 h. Stock solutions of the complexes were prepared in water for cisplatin and in DMSO for the platinum and bimetallic compounds. The percentage of DMSO in the culture medium did not exceed 1%. After 72 h, the medium was removed and the cells were incubated with MTT solution in PBS (10 µL of a 5 mg/mL) for 2-3 h of incubation. The formed purple formazan crystals were dissolved in 100 µL of DMSO by thorough shaking, and the absorbance at 560 nm was read using a plate spectrophotometer (FLUOstar OPTIMA). Each test was performed with at least 3 replicates and repeated at least 3 times. The IC_{50} value is determined using GraphPad Prism 8.0 software.

Acknowledgements

The work was financially supported by Sorbonne Université and CNRS. The Fédération de Recherche (FR2769) provided technical access for analysis. B. B. thanks Aurélie Bernard, Claire Troufflard for their help for NMR analyzes and Dr. Cédric Przybylski for the HR-MS analyzes. B. B. thanks Dr. Patricia Forgez for providing A2780 and MCF-10A cells which she got from ATCC.

Keywords

Bioorganometallic chemistry, heterobimetallic complexes, platinum, synthesis, cancer

References

[1] M. Watson, A. Barrett, R. Spence, C. Twelves, *Oncology*, Oxford University Press, Oxford, 2nd edn, **2006**

[2] R. Oun, Y. E. Moussa and N. J. Wheate, *Dalton Trans.,* 2018, **47**, 6645-6653.

[3] M. Wenzel, B. Bertrand, M.-J. Eymin, V. Comte, J. A. Harvey, P. Richard, M. Groessl, O. Zava, H. Amrouche, P. D. Harvey, P. Le Gendre, M. Picquet, A. Casini, *Inorg. Chem.* **2011**, *50*, 9472-9480

[4] L. K. Batchelor, D. Ortiz, P. J. Dyson, *Inorg. Chem.,* **2019**, *58*, 2501-2513.

[5] M. Wenzel, E. Bigaeva, P. Richard, P. Le Gendre, M. Picquet, A. Casini, E. Bodio, *J. Inorg. Biochem.,* **2014**, *141*, 10-16.

[6] S. Jovanović, K. Obrenčević, Ž. D. Bugarčić, I. Popović, J. Žakulac, B. Petrović, *Dalton Trans.,* **2016**, *45*, 12444-12457.

[7] P. De Hoog, M. Pitié, G. Amadei, P. Gamez, B. Meunier, R. Kiss, J. Reedijk, *J. Biol. Inorg. Chem.,* **2008**, *13*, 575-586

[8] V. Ramu, M. R. Gill, P. J. Jarman, D. Turton, J. A. Thomas, A. Das, C. Smythe, *Chem. Eur. J.,* **2015**, *21*, 8185-8197.

[9] B. Bertrand, J. Forté, C. Botuha, H. Dossmann, M. Salmain, **2020**, DOI: 10.1002/chem.202001752.

[10] (a) B. Bertrand, P.-E. Doulain, C. Goze, E. Bodio, *Dalton Trans.,* **2016**, *45*, 13005-13011. (b) V. Fernández-Moreira, M. C. Gimeno, *Chem. Eur. J.,* **2018**, *24*, 3345-3353.

[11] (a) V. Fernández-Moreira, I. Marzo, M. C. Gimeno, *Chem. Sci.,* **2014**, 5, 4434-4446. (b) L. Boselli, M. Carraz, S. Mazères, L. Paloque, G. González, F. Benoit-Vical, A. Valentin, C. Hemmert, H. Gornitzka, *Organometallics,* **2015**, 34, 1046-1055.

[12] Z. Zhu, X. Wang, T. Li, S. Aime, P. J. Sadler, Z. Guo, *Angew. Chem. Int. Ed.,* **2014**, *53,* 13225-13228.

[13] (a) M. G. Mendoza-Ferri, C. G. Hartinger, M. A. Mendoza, M. Groessl, A. E. Egger, R. E. Eichinger, J. B. Mangrum, N. P. Farrell, M. Maruszak, P. J. Bednarski, F. Klein, M. A. Jakupec, A. A. Nazarov, K. Severin, B. K. Keppler, *J. Med. Chem.,* **2009**, *52*, 916-925. (b) M. Serratrice, F. Edafe, F. Mendes, R. Scopelliti, S. M. Zakeeruddin, M. Grätzel, I. Santos, M. A. Cinellu, A. Casini, *Dalton Trans.* **2012**, *41*, 3287-3293. (c) R. W. Y. Sun, C. N. Lok, T. T. H. Fong, C. K. L. Li, Z.F. Yang, T. T. Zou, A. F. M. Siu, C.-M. Che, *Chem. Sci.,* **2013**, *4*, 1979-1988.

[14] (a) F. Pelletier, V. Comte, A. Massard, M. Wenzel, S. Toulot, P. Richard, M. Picquet, P. Le Gendre, O. Zava, F. Edafe, A. Casini, P. J. Dyson, *J. Med. Chem.,* **2010**, *53*, 6923-6933. (b) J. Fernandez-Gallardo, B. T. Elie, T. Sadhukha, S. Prabha, M. Sanau, S. A. Rotenberg, J. W. Ramos, M. Contel, *Chem. Sci.*, **2015**, *6*, 5269-5283.

[15] (a) B. Bertrand, E. Bodio, P. Richard, M. Picquet, P. Le Gendre, A. Casini, *J. Organomet. Chem.,* **2015**, *775*, 124-129. (b) M. Wenzel, A. de Almeida, E. Bigaeva, P. Kavanagh, M. Picquet, P. Le Gendre, E. Bodio, A. Casini, *Inorg. Chem.,* **2016**, *55*, 2544-2557. (c) B. Bertrand, M. A. O'Connell, Z. A. E. Waller, M. Bochmann, *Chem. Eur. J.,* **2018**, *24*, 3613-3622.

[16] R. E. Morris, R. E. Aird, P. del Socorro Murdoch, H. Chen, J. Cummings, N. D. Hughes, S. Parsons, A. Parkin, G. Boyd, D. I. Jodrell, P. J. Sadler, *J. Med. Chem.,* **2001**, *44*, 3616-3621.

[17] J. M. Hearn, I. Romero-Canelón, B. Qamar, Z. Liu, I. Hands-Portman, P. J. Sadler, *ACS Chem. Biol.,* **2013**, *8*, 1335-1343.

[18] M.-L. Teyssot, A.-S. Jarrousse, A. Chevry, A. De Haze, C. Beaudoin, M. Manin, S. P. Nolan, S. Díez-González, L. Morel, A. Gautier, *Chem. Eur. J.* **2009**, *15*, 314-318.

[19] B. Bertrand, A. Citta, I. L. Franken, M. Picquet, A. Folda, V. Scalcon, M. P. Rigobello, P. Le Gendre, A. Casini, E. Bodio, *J. Biol. Inorg. Chem.,* **2015**, *20*, 1005-1020.

[20] V. A. Krylova, P. I. Djurovich, M. T. Whited, M. E. Thompson, *Chem. Commun.,* **2010**, *46*, 6696-6698.

[21] K. Brandenburg, **1999**, DIAMOND. Crystal Impact GbR, Bonn, Germany

[22] F. Wang, H. Chen, S. Parsons, I. D. H. Oswald, J. E. Davidson, P. J. Sadler, *Chem. Eur. J.,* **2003**, *9*, 5810-5820.

[23] D. J. Minick, J. H. Frenz, M. A. Patrick and D. A. Brent, *J. Med. Chem.,* **1988**, *31*, 1923–1933.

[24] J. M. Zimbron, K. Passador, B. Gatin-Fraudet, C.-M. Bachelet, D. Plażuk, L.-M. Chamoreau, C. Botuha, S. Thorimbert**,** M. Salmain, *Organometallics*, **2017**, *36*, 3435-3442.

[25] H. Yao, G. He, S. Yan, C. Chen, L. Song, T. J. Rosol, X. Deng, *Oncotarget,* **2017**, *8*, 1913-1924.

[26] F. Ciardello, Rosa Caputo, G. Pomatico, M. De Laurentiis, S. De Placido, A. R. Bianco, G. Tortora, *Int. J. Cancer,* **2000**, *85*, 710-715.

[27] M. Elie, F. Sguerra, F. Di Meo, M. D. Weber, R. Marion, A. Grimault, J.-F. Lohier, A. Stallivieri, A. Brosseau, R. B. Pansu, J.-L. Renaud, M. Linares, M. Hamel, R. D. Costa, S. Gaillard, *ACS Appl. Mater. Interfaces,* **2016**, *23*, 14678-14691.

TOC Graphic

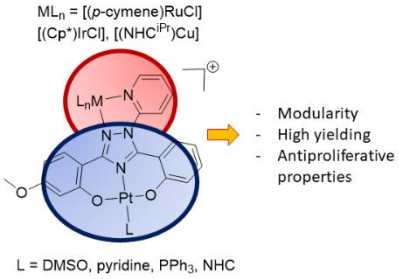

Key topic : bioorganometallic, cancer

The use of an [(O^N^O)PtL] platform bearing a free (N^N) ligand opened the way to the synthesis of various heterobimetallic complexes Pt/Ru, Pt/Ir and Pt/Cu which demonstrated interesting antiproliferative properties *in vitro.*